The moment magnitude and the energy magnitude: common roots and differences

Peter Bormann, Domenico Giacomo

The moment magnitude M_w and the energy magnitude M_e: common roots and differences

by
Peter Bormann and Domenico Di Giacomo*
GFZ German Research Centre for Geosciences, Telegrafenberg, 14473 Potsdam, Germany
*Now at the International Seismological Centre, Pipers Lane, RG19 4NS Thatcham, UK

Abstract

Starting from the classical empirical magnitude-energy relationships, in this article the derivation of the modern scales for moment magnitude M_w and energy magnitude M_e is outlined and critically discussed. The formulas for M_w and M_e calculation are presented in a way that reveals, besides the contributions of the physically defined measurement parameters seismic moment M_0 and radiated seismic energy E_S, the role of the constants in the classical Gutenberg-Richter magnitude-energy relationship. Further, it is shown that M_w and M_e are linked via the parameter $\Theta = \log(E_S/M_0)$, and the formula for M_e can be written as $M_e = M_w + (\Theta + 4.7)/1.5$. This relationship directly links M_e with M_w via their common scaling to classical magnitudes, and, at the same time, highlights the reason why M_w and M_e can significantly differ. In fact, Θ is assumed to be constant when calculating M_w.

However, variations over three to four orders of magnitude in stress drop $\Delta\sigma$ (as well as related variations in rupture velocity V_R and seismic wave radiation efficiency η_R) are responsible for the large variability of actual Θ values of earthquakes. As a result, for the same earthquake M_e may sometimes differ by more than one magnitude unit from M_w. Such a difference is highly relevant when assessing the actual damage potential associated with a given earthquake, because it expresses rather different static and dynamic source properties. While M_w is most appropriate for estimating the earthquake size (i.e., the product of rupture area times average displacement) and thus the potential tsunami hazard posed by strong and great earthquakes in marine environs, M_e is more suitable than M_w for assessing the potential hazard of damage due to strong ground shaking, i.e., the earthquake strength. Therefore, whenever possible, these two magnitudes should be both independently determined and jointly considered. Usually, only M_w is taken as a unified magnitude in many seismological applications (ShakeMap, seismic hazard studies, etc.) since procedures to calculate it are well developed and accepted to be stable with small uncertainty. For many reasons, procedures for E_S and M_e calculation are affected by a larger uncertainty and are currently not yet available for all global earthquakes. Thus, despite the physical importance of E_S in characterizing the seismic source, the use of M_e has been limited so far to the detriment of quicker and more complete rough estimates of both earthquake size and strength and their causal relationships. Further studies are needed to improve E_S estimations in order to allow M_e to be extensively used as an important complement to M_w in common seismological practice and its applications.

Introduction

The moment magnitude M_w, as proposed and developed by Kanamori (1977) and Hanks and Kanamori (1979), is often considered as the only physically well defined, non-saturating magnitude scale and estimator of the earthquake size. The methodology of M_w determination is rather well developed and routinely practised in a standardized way since 1976 as a spin-off of the Harvard procedure of Centroid-Moment-Tensor solutions (Dziewonski et al., 1981). In contrast, the classical magnitude scales for local (M_L, Richter, 1935) and teleseismic earthquakes (m_B and M_S, Gutenberg, 1945a, b, and c; Gutenberg and Richter, 1956a), as well as a host of later introduced complementary or modified versions of them, are measured in different period and bandwidth ranges, often with incompatible procedures that sometimes even have changed with time (Bormann et al., 2007 and 2009; Bormann and Saul, 2009a). This is most inappropriate for intermediate and long-term probabilistic seismic hazard assessment. Therefore, it has become widespread practice to convert traditional local or teleseismic magnitude values via empirical regression relationships into "equivalent" M_w values (e.g., Papazachos et al., 1997, Stromeyer et al., 2004; Ristau et al., 2005, Scordilis, 2006). This practice aims at the compilation of homogeneous, with respect to magnitude, earthquake catalogs suitable for intermediate- and long-term seismic hazard assessment with M_w as the unified parameter to characterize earthquake size (e.g., Grünthal and Wahlström, 2003, Braunmiller et al., 2005, Grünthal et al., 2009). Although understandable in view of the often confusing inhomogeneity of different magnitude data sets and lacking standards in traditional earthquake catalogues, this approach is generally too simple and physically not justified. Therefore, at least when assessing the hazards associated with actual earthquakes, it should be replaced by a knowledgeable use of different complementary magnitudes that have been determined on the basis of modern measurement procedures and standards,.

According to numerous authors (e.g., Kanamori, 1977 and 1983; Choy and Boatwright, 1995; Bormann et al., 2002; Kanamori and Brodsky, 2004; Bormann and Saul, 2008 and 2009; Bormann et al., 2009; Yadav et al., 2009; Di Giacomo et al., 2010a and b) a single magnitude practice overlooks the following considerations:

a) That the moment magnitude M_w, derived via the static seismic moment M_0, is only a static measure of earthquake "size", i.e., of the average tectonic effect of an earthquake. M_0 depends on the difference in strain energy before and after an earthquake. Thus its value relates to the total non-elastic "work" W performed in the source volume but not on the actual time history of the faulting itself.

b) Accordingly, M_w and M_0 do not provide direct information about the comparatively small fraction of released elastic wave energy E_S and its dominant frequency content. The latter, however, is largely controlled by the dynamic and kinematic characteristics of the rupture process and thus is highly relevant for assessing the actual damage potential associated with seismic energy radiated by an earthquake.

c) That this inherent limitation of M_w can only be overcome by a multi-magnitude approach based on measurements in different hazard-relevant frequency ranges.

d) For estimating the potential shake-damage of actual earthquakes, local magnitudes based on high-frequency and/or strong-motion amplitude measurements are particularly useful for producing shake maps. In reality, most earthquake-prone countries do not yet avail of the required dense and online operated strong-motion networks on their own territories. Such countries still have to rely on near real-time magnitude information provided by regional and global data centres that use modern broadband records, mostly within the teleseismic distance range.

e) Broadband records allow for the measurement of both moment magnitude M_w, based on long-period displacement data, and energy magnitudes M_e, based on ground motion velocity data over a wide range of periods. Both M_w and M_e are comparably well defined in a physical sense. It is their joint consideration which allows a more realistic quick assessment of the kind and seriousness of seismic hazard associated with an actual earthquake than M_w alone.

Therefore, we will look in this paper into both the common roots and physical differences of M_w and M_e, how they relate to fundamental classical magnitude standards, and how these two magnitudes could be used jointly in quick rough assessment of the earthquake's damage potential.

How was M_w derived?

Gutenberg and Richter (1956a) published the following standard regression relation between medium-period body-wave magnitude m_B, measured at periods between about 2 and 20 s (see Abe, 1981) and surface-wave magnitude M_S measured at periods around 20 s:

$$m_B = 0.63\, M_S + 2.5 \tag{1}$$

and between m_B and released seismic energy E_S:

$$\log E_S = 2.4\, m_B - 1.2 \tag{2}$$

(if E_S is given in J = Joule and log = $\log_{10}$). The semi-empirical relationship (2) is just a rough estimate with no error calculation through only 20 data points of different origin in the magnitude range $2 \leq m_B \leq 8.0$ and E_S has been estimated by the authors on the basis of an equation for a wave group from a point source with magnitude-dependent amplitude and waveform duration (Gutenberg and Richter, 1956b, and Figure 1 therein).

In the paper "The energy release in great earthquakes", in which Kanamori (1977) intended to estimate via known scalar seismic moments M_0, the following relationship is given between the strain energy drop W and M_0 for the case of "*complete stress drop*" $\Delta\sigma$ in the source and with μ = average rigidity of the medium in the source area:

$$W = W_0\ (=E_S) = (\Delta\sigma/2\mu)\, M_0. \tag{3}$$

However, as explained in more detail in later sections herein on the physical basis of Eq.(3), the latter is valid only under the assumptions that during earthquake rupture a) the energy required for fracturing is negligible and b) the finally reached stress is equal to the stress due to kinematic friction ("complete stress drop*",* Orowan, 1960). However, the rupture process may deviate from these conditions, as discussed already by Brune (1970; "partial stress drop") or by Savage and Wood (1971¸"frictional overshoot").

Further, Kanamori assumed $\mu = 3\text{-}6 \times 10^{11}$ dyn/cm^2 = $3\text{-}6 \times 10^4$ MPa in the source area under average crust-upper mantle conditions, and on the basis of elastostatic considerations (as earlier Knopoff, 1958) that also the *stress drop is nearly constant* with values between some 20 and 60 bars = $2\text{-}6 \times 10^7$ dyn/cm^2 = 2-6 MPa *for very large earthquakes*. Users of the moment magnitudes scale in a much wider range down to magnitude 3 (Braunmiller et al., 2002), 1 (Abercrombie, 1995) or even -4.4 (Kwiatek et al., 2010) seem not to be aware of, or do not question, these underlying assumptions, which lead via Eq. (3) to

$$E_S = W_0 \approx M_0/(2 \times 10^4) \tag{4}$$

or

$$E_S/M_0 = 5 \times 10^{-5} = \text{constant}. \tag{5}$$

Thus, if all these conditions were correct, one could easily calculate E_S from known M_0 via Eq. (5). Kanamori (1977) used this equation to introduce the non-saturating moment-magnitude scale M_w. For practical applications M_w is a more convenient measure for the overall deformation at the source and thus of the "size" of great earthquakes than

$$M_0 = \mu\, S\, D \propto u_0 \tag{6}$$

(where S = rupture surface, D = displacement averaged over the rupture surface, and u_0 = asymptotic long-period displacement amplitude of the source spectrum), because values of M_0 range over many decades.

In order to scale M_0 to magnitude, an energy-magnitude relationship was required. Yet, Eq. (2) was not suitable for this purpose anymore, since medium-period broadband m_B was no longer measured at western seismological stations and data centers after the global deployment of the US World-Wide Standard Seismograph System (WWSSN) in the 1960s. Therefore, Kanamori followed the proposal by Richter (1958) to insert Eq. (1) into (2) which yields:

$$\log E_S = 1.5M_S + 4.8. \quad (7)$$

This is the commonly referred to and most widely used "Gutenberg-Richter" energy-magnitude relationship".

However, theoretical considerations by Kanamori and Anderson (1975) indicated that $\log E_S \propto 1.5M_S$ holds *for moderate to large earthquakes*, that energy estimates from M_S via Eq. (7) agree in this range fairly well with the static estimates according to Eq. (5) (see also Vassiliou and Kanamori, 1982) but that M_S tends to saturate for really great earthquakes, as strikingly documented by the great 1960 Chile (M_S = 8.3) and 1964 Alaska earthquake (M_S = 8.5). Therefore, Kanamori substituted M_S in the $\log E_S$-M_S relationship with the symbol M_w for the envisaged non-saturating moment (or "work") magnitude. When using the above relationships in international standard units, one arrives via Eq. (5) at

$$\log E_S = \log M_0 - 4.3 = 1.5M_w + 4.8, \quad (8)$$

and when resolving it for M_w:

$$M_w = (\log M_0 - 4.3 - 4.8)/1.5 = (\log M_0 - 9.1)/1.5. \quad (9)$$

Eq. (9) is identical with the IASPEI (2005) standard formula $M_w = (2/3)(\log M_0 - 9.1)$, first proposed by Bormann et al. (2002). This equation avoids occasional differences of 0.1 magnitude units (m.u.) between M_w values calculated for identical M_0 with a precision of one decimal caused by the too early rounding-off of the constant in the original M_w formula published by Hanks and Kanamori (1979). When introducing the parameter $\Theta = \log(E_S/M_0)$ (termed "slowness parameter" by Okal and Talandier, 1989), the Kanamori condition (5) reduces to Θ_K = -4.3 = constant and Eq. (9) reads via Eq. (8):

$$M_w = (\log M_0 + \Theta_K - 4.8)/1.5. \quad (10)$$

This way of writing reveals best both the physics and the classical empirical roots of M_w:

- 1.5 corresponds to the slope of the $\log E_S$-M_S relationship (7) that has been derived via Eqs. (1) and (2);
- 4.8 is the constant in relationship (7) and
- Θ_K = -4.3 = constant results from Eq. (3) and the assumptions made by Kanamori (1977) on $\Delta\sigma$ and μ.

Physically, a "constant-stress-drop" scaling of an earthquake source-spectrum would mean that the low-frequency content of the spectrum, which controls M_0, would also control the high-frequency content, which chiefly contributes to the radiated seismic energy E_S (see Figure 1 in the last but one section).

This is, in fact, the oversimplified concept of seismic scaling according to Aki (1967), namely that the entire source spectrum could be specified by just one parameter such as seismic moment or a unique magnitude. However, as spelled out earlier, e.g. by Kanamori (1978, 1983), Duda and Kaiser (1989), Bormann et al. (2002), a single magnitude cannot describe essential differences in source characteristics. Beresnev (2009) also emphasises that earthquake dislocation is controlled, even in the simplest case, by at least two independent parameters, namely 1) the final static offset and 2) the speed at which it is reached. The former controls the low-frequency asymptote of the spectrum, whereas rupture speed and stress drop essentially control the position of the source-spectrum´s corner frequency f_c and thus the high-frequency content of the radiated spectrum (compare Figs. 1 and 2). These differences necessitate the development of an energy magnitude which is based on direct calculations of E_S from the seismic records, thus being free of presuppositions such as constant rigidity, stress drop and/or rupture velocity.

How was M_e derived?

Choy and Boatwright (1995) scaled the energy magnitude M_e to M_S in a similar way as Kanamori (1977) scaled M_w with the Gutenberg-Richter relationship (7). However, instead of making assumptions about the ratio E_S/M_0, they calculated Es directly by integrating squared broadband velocity amplitudes over the duration of the *P*-wave train and corrected the integral for wave propagation and source radiation pattern effects based on suitable Earth and source models. Then they plotted for hundreds of earthquakes $\log E_S$ over the respective M_S values between 5.5 and 8.3 and determined from a standard least-square regression the best fitting straight line with the prescribed slope of 1.5 as in Eq. (7). Thus, however, they found instead of the constant 4.8 in relation (7) the constant 4.4 that yielded a better average fit through the data cloud. Nevertheless, Choy and Boatwright decided in their 1995 paper: “For consistency with historical computations as well as with other types of magnitude that have been derived from the Gutenberg-Richter formula, we retain the original constants”. Thus they arrived at

$$M_e = (2/3)\log E_S - 3.2 = (\log E_S - 4.8)/1.5 \qquad (11)$$

with E_S in units of Joule. Note: If this mutual scaling of M_w and M_e with Eq. (7) would have been kept, and if $\Theta av = \Theta_K$ would indeed hold on a global average, then the mean difference between M_w and M_e would be zero for a representative global event data set. The latter, however, is not the case. Therefore Choy and Boatwright reverted in subsequent papers to the better fitting constant of 4.4 and changed Eq. (11) to

$$M_e = (2/3)\log E_S - 2.9. \qquad (12)$$

Until recently, Eq. (12) has been used to calculate the M_e values published by the US Geological Survey´s National Earthquake Information Center (NEIC). Yet this same equation still had the same problem of too early rounding-off the constant (which should be 2.9333… instead of 2.9) as the original M_w formula published by Hanks and Kanamori (1979). This can be avoided by starting from the best fitting regression to real data in Choy and Boatwright (1995),

$$\log E_S = 1.5M_S + 4.4, \qquad (13)$$

replacing M_S by M_e and resolving it for M_e. This yields

$$M_e = (2/3)(\log E_S - 4.4) = (\log E_S - 4.4)/1.5. \qquad (14)$$

First proposed by Bormann et al. (2002), Eq. (14) is equivalent with the writing of Eq. (9) for M_w and now is accepted as standard also at the NEIC/USGS.

How do the formal definitions for M_w and M_e physically relate to each other?

According to the above line of deductions, the energy/moment ratio E_S/M_0 is evidently a very useful parameter that characterizes the dynamic properties of an earthquake (Aki, 1966; Wyss and Brune, 1968). Kanamori and Brodsky (2004) termed it "scaled energy", which is in fact the seismic energy radiated per unit of moment release. According to (3) it holds

$$E_S/M_0 = \Delta\sigma/2\mu = \tau_a/\mu \tag{15}$$

with τ_a = apparent stress according to Wyss and Brune (1968), which can also be written as $\tau_a = E_S/(D \cdot S)$. Thus, τ_a is equivalent to the seismic energy release per unit area of the ruptured surface times slip.

In order to make the physical relationship between M_w and M_e according to the above stated conditions better tractable, one should write (14) in a form that is comparable with (9) and (10) in order to reveal the dependence on rigidity, stress drop and apparent stress, respectively. From $E_S/M_0 = 10^{\Theta}$ follows

$$\log E_S = \log M_0 + \Theta. \tag{16}$$

Inserting (16) in (14) yields

$$M_e = (\log M_0 + \Theta - 4.4)/1.5 \tag{17}$$

and through a few more steps one arrives at

$$\boldsymbol{M_e = M_w + (\Theta + 4.7)/1.5 = M_w + [\log(E_S/M_0) + 4.7]/1.5} \tag{18a}$$
$$= M_w + [\log(\Delta\sigma/2\mu) + 4.7]/1.5 \tag{18b}$$
$$= M_w + [\log(\tau_a/\mu) + 4.7]/1.5. \tag{18c}$$

Eq. (11) in the paper by Choy and Boatwright (1995) is essentially equivalent with eq. (18c), however with other constants, because it was still derived via Eq. (7) instead of (13), and it expresses E_S in terms of M_0 instead of M_w.

By comparing Eqs. (10) and (17), it becomes very obvious why M_w and M_e differ. First, there is a constant offset of 0.27 m.u. due to the different constants in the brackets, namely 4.8 and 4.4. Moreover, there is a variable difference, namely that between $\Theta_K = -4.3$ = constant and the highly variable real Θ of earthquakes, which may range between about -3.2 and -6.9 (e.g., Choy et al., 2006; Weinstein and Okal, 2005; Lomax and Michelini, 2009a). This explains possible differences between M_w and M_e by more than a magnitude unit.

Eq. (18a-c) may be helpful for calculating values of Θ, or the dimensionless ratios E_S/M_0, $\Delta\sigma/2\mu$ or τ_a/μ, respectively, but only when M_w and M_e have been reported for a given earthquake. From (18a) it is also obvious that $M_w = M_e$ holds true only for earthquakes with $\Theta = -4.7$. But in no event should these equations be used for converting M_w into M_e or vice versa. Their purpose is only to show what makes the difference between these two magnitudes, under what condition they are equal, how different they may become and what are likely physical reasons for their difference.

According to Eq. (18b) there is a trade-off between changes in $\Delta\sigma$ and μ. For μ = constant holds $E_S \approx \Delta\sigma\ S\ D/2$ (Kostrov, 1974), i.e., for a given seismic moment M_0, E_S varies proportional to stress drop $\Delta\sigma$. $M_e = M_w$ corresponds to a stress drop of $\Delta\sigma \approx 1.2$ to 2.4 MPa if Kanamori´s (1977) assumption of μ = const. $\approx 3\text{-}6 \times 10^4$ MPa is valid. However, with $\Theta = \Theta_K = -4.3$, (18a) yields $M_e = M_w + 0.27$ and a 2.5 times larger stress drop, as assumed by Kanamori (1977). This is rarely the case and surely not the average condition for earthquakes reported in the USGS SOPAR database (http://neic.usgs.gov/neis/sopar/). This indicates that Eq. (5) assumes a larger than empirically measured average ratio $\Delta\sigma/\mu$ and related E_S. In fact, average values of Θ for different global data sets of earthquakes with M_w between about 5.5 and 9 vary between -4.7 and -4.9 (Choy and Boatwright, 1995; Choy et al., 2006; Weinstein and Okal, 2005). Accordingly, on average one can expect M_e to be close to or somewhat smaller than M_w. If one accepts $\Theta = -4.9$ as being most representative and, according to Weinstein and Okal, also in good agreement with established scaling laws, than this would correspond to an average global stress drop of only about 0.8 to 1.5 MPa, i.e., a factor 3 to 4 less than assumed by condition (5). This necessitates looking into the theoretical reasons which could explain these discrepancies. Moreover, since according to Eqs. (18a) and (18b)

$$\log(\Delta\sigma/2) = \log\tau_a = \log\mu + \Theta, \tag{19}$$

calculations of stress drop or apparent stress require to know besides Θ also the rigidity μ in the source volume sufficiently well. Yet uncertainties may be much larger than the factor of 2, which Kanamori (1977) had already accounted for. Especially in the case of slow tsunami earthquakes (Polet and Kanamori, 2000 and 2009) one has to assume much smaller rigidity values than for average crustal-upper mantle conditions. Tsunami earthquakes generate by definition much larger tsunami than expected from their respective M_w, and M_0 values, most likely due to abnormally low rigidity along the rupture surfaces of shallow earthquakes in some shallow dipping marine subductions zones (Houston, 1999). In such cases – according to Eq. (6) – the product $S \cdot D$ and thus the generated tsunami has for a given M_0 to be larger in order to compensate for the smaller μ. This illustrates the range of uncertainty in estimating M_w due to average assumptions made in deriving the M_w formula.

Why do estimates of E_S via Eqs. (3) to (5) tend to overestimate $\Delta\sigma$ and E_S?

When introducing the Kanamori (1977) relationship (3) in this paper, we indicated that this relationship is based on simplified assumptions about the rupture process because it does not yet consider the total energy balance of the rupture process, as later done by Kanamori and Brodsky (2004). Using their notations, namely E_R for radiated seismic energy (instead of the traditional E_S), E_G for the fracture energy and E_H for the energy dissipated as heat due to kinematic friction on the fault, then the total change in potential energy due to the rupture process can be written as

$$\Delta W = E_R + E_G + E_H\ . \tag{20}$$

If the initial stress prior to rupturing is σ_0 and the final stress reached after rupturing σ_1, which corresponds to a stress drop $\Delta\sigma = \sigma_0 - \sigma_1$, then the potential deformation energy at the source is

$$\Delta W = (\sigma_0 + \sigma_1) D \cdot S/2. \tag{21}$$

Further, with σ_f the kinematic friction, the frictional energy is

$$E_H = \sigma_f D S. \quad (22)$$

Kanamori and Brodsky (2004) then introduced the quantity $\Delta W_0 = \Delta W - E_H$, which is the difference between total change in potential energy and frictional energy. Inserting this into equation (20) yields $\Delta W_0 = E_R + E_G$, being the potential energy available for strain release, termed ΔE_{T0} in a later publication by Kanamori (2006).

With the condition by Kanamori (1977 for deriving Eq. (3), i.e., $\sigma_1 \approx \sigma_f$, one can replace in Eq. (22) σ_f by σ_1. When then inserting E_H in $\Delta W_0 = \Delta W - E_H$ one arrives with Eqs. (21) and (6) at

$$\Delta W_0 = \Delta\sigma D S/2 = (\Delta\sigma/2\mu) M_0 . \quad (23)$$

This is equivalent to Eqs. 3.14 – 3.16 and 4.36 in Kanamori and Brodsky (2004), with the right side being identical with Eq. (3). However, $E_S = E_R = \Delta W_0$ holds only for $E_G = 0$, i.e., when neglecting the fracture energy E_G in the total energy budget. Generally, however, the radiated energy is less, namely

$$E_R = \Delta W_0 - E_G. \quad (24)$$

Husseini (1977) introduced the term of radiation efficiency

$$\eta_R = E_R/(E_R + E_G). \quad (25)$$

According to Kanamori (2006), Eq. (25) can also be written as

$$\eta_R = (2\mu/\Delta\sigma)(E_R/M_0) = E_R/\Delta E_{T0} = (E_R/\Delta W_0) \quad (26)$$

Then it becomes clear that $E_S = E_R = (\Delta\sigma/2\mu)M_0$ holds only for $\eta_R = 1$, i.e., when all energy available for strain release is converted into seismic wave energy, and no energy E_G is dissipated during fracturing.

In this context it has to be clarified, however, that *radiation efficiency* η_R according to Eq. (25) should not be mistaken as the better known *seismic efficiency* η, which additionally accounts for the energy loss due to frictional heat E_H):

$$\eta = E_R/(E_R + E_G + E_H) \quad (27)$$

and, thus, is significantly smaller than η_R.

Which other parameters besides $\Delta\sigma$ and μ may strongly influence radiation efficiency?

So far we have only discussed the influence of variations in stress drop, respectively $\Delta\sigma/\mu$, on the ratio E_S/M_0 according to the formulas that were used to define M_w and M_e. But according to Newman and Okal (1998), even in the case of a kinematically simple rupture model this ratio is controlled by five dimensionless factors, namely the ratios (with different exponent) between 1) S- versus P-wave velocity, 2) rupture length versus rupture duration and Rayleigh-wave speed, 3) rupture velocity V_R versus shear-wave velocity β, 4) rupture width versus rupture length (i.e., the aspect ratio), and 5) fault slip versus rupture width. Moreover, one has to be aware that especially in the case of large complex earthquakes, the amount and frequency content of radiated seismic energy is not chiefly controlled by the mean rupture velocity, stress drop and fault displacement over the whole fault, but rather by the respective values related to the braking of asperities, i.e., of major stress or rigidity/friction anomalies along the fault. Yet handling and determining so many parameters with sufficient reliability is usually not possible, and in no event in near real time. Therefore in the following we look only into one of these factors, namely the ratio V_R/β, because there are possibilities of near real-time estimates of V_R with recently developed procedures (e.g., Krüger and Ohrnberger, 2005). According to Venkataraman and Kanamori (2004a), both theory and empirical data confirm (although the latter only with great scatter) a trend of growing η_R with increasing V_R/β. The ratio may vary between about 0.2 to 0.95, yet being > 0.6 for most of the large earthquakes so far analyzed.

According to Kostrov (1966) and Eshelby (1969) it holds for transverse shear cracks that $\eta_R \approx (V_R/\beta)^2$. Inserting this into Eq. (26) and resolving it for the ratio E_S/M_0 yields

$$E_S/M_0 = \eta_R \cdot (\Delta\sigma/2\mu) \approx (V_R/\beta)^2 \cdot (\Delta\sigma/2\mu). \qquad (28)$$

Although being model-dependent (and other models are likely to produce other relationships), Eq. (28) illustrates a trade-off between variations in stress drop, rigidity, rupture velocity and shear-wave velocity, which may control the ratio E_S/M_0 and, thus, the relationship between M_w and M_e.

Data that confirm both trend and individual event differences between M_w and M_e

The general assumption that $\eta_R = 1$ is not realistic. Published values of η_R (Venkataraman and Kanamori, 2004a; Kanamori and Brodsky, 2004; Kanamori, 2006) show large scatter due to uncertainties in the determination of E_S, M_0 and $\Delta\sigma$, as well as the limitations of the slip-weakening model assumed to calculate the partitioning of energy in earthquakes. For most earthquakes η_R ranges between 0.25 and 1, although smaller values - down to about 0.02 - have been determined as well. Strike-slip earthquake tend to have, on average, the largest radiation efficiencies, yielding typically values $M_e > M_w$ and the largest values of apparent stress or stress-drop inferred therefrom (e.g., Choy and Boatwright, 1995; Choy et al., 2004). The lowest values of η_R were found for tsunami earthquakes, for which generally holds that $M_e << M_w$ (see below). The great 2004 Sumatra-Andaman earthquake ranged with an average value of $\eta_R = 0.16$ between tsunami earthquakes and "normal" earthquakes. However, values have been significantly larger in the first rupture segment and dropped down to about 0.05, or even less, in the last two major rupture segments (Kanamori, 2006). Interestingly, the average value $\eta_R = 0.16$ (as compared to $\eta_R = 1$ for complete stress drop) would already fully explain the difference between M_e(USGS) = 8.5 and M_w(GCMT) = 9.0 for this Sumatra earthquake. In summary:

- The radiation efficiency of earthquakes and thus their ratio E_S/M_0 varies over a wide range and may vary even within a given rupture process;
- The condition $E_S/M_0 = 5 \times 10^{-5}$ = const., on which the definition of the moment magnitude rests, would yield E_S estimates via M_0 that are on average a factor of 2-3 times too large. Therefore, with procedures for direct energy estimates now being readily available (see next section) this condition should no longer be used for such estimates.
- The range of radiation efficiency variations explains the observed differences between M_w and M_e, which may reach more than ± 1 m.u. for the same event.

Very obvious is the influence of the rupture velocity in the case of tsunami earthquakes, e.g. the 1992 M_w 7.6 Nicaragua earthquake with M_e = 6.7 and the more recent 2006 M_w 7.7 Java earthquake with M_e = 6.8. Moment-wise, both earthquakes are comparably large, yet their rupture durations T_R range between about 100 s and 220 s (Kanamori and Kikuchi, 1993; Hara, 2007b; Lomax and Michelini, 2009a; Bormann and Saul, 2008 and 2009b). According to the relationship $T_R \approx 0.6M - 2.8$ by Bormann et al. (2009),this is about 2-4 times longer than expected on average for earthquakes of the same moment magnitude.

Other striking examples for differences between M_w and M_e are the 2 June 1994 M_w 7.8 Java tsunami earthquake where much smaller values were reported for M_e (6.5-6.8). This strongly contrasts with $M_e >> M_w$, e.g. the 15 October 1997 M_w 7.1 Chile earthquake (Choy and Kirby, 2004) and the 12 January 2010 M_w 7.1 Haiti earthquake with M_e values of 7.5 and 7.6, respectively, associated with major devastations due to strong shaking. More examples are given by Di Giacomo et al. (2010a and b).

In the following we look into the different approaches and related uncertainties in calculating M_0 and E_S values, each of which are the "measured" input parameters for M_w and M_e calculations respectively.

Essential differences in measuring and calculating M_0 and E_S

The basic procedures for calculating ("measuring") M_0 and E_S have been outlined in many publications, e.g., Dziewonski et al. (1981), Boatwright and Choy (1986), Choy and Boatwright (1995), Bormann et al. (2002), Di Giacomo et al. (2010a,b). They will not be repeated here. Most important, however, is to note that the wave amplitudes measured, fitted with synthetics, or integrated when determining M_0 or E_S, respectively, relate to rather different period and bandwidth ranges. This is illustrated with respect to the classical earthquake magnitudes m_b, m_B and M_S in Fig. 1. This figure depicts seismic displacement and velocity source spectra scaled to seismic moment and moment rate, respectively, for model earthquakes with M_w in the range from 4 to 9. The spectral curves (solid lines) have been calculated with an ω^{-2} source model (Aki, 1967, 1972). The Fourier transform of the moment rate function can then be expressed as $\hat{\dot{M}}(f) = (M_o f_c^2)/(f^2 + f_c^2)$ (Houston and Kanamori, 1986; Polet and Kanamori, 2000) with the corner frequency f_c depending on stress drop and seismic moment according to the relationship given by Brune (1970)

$$f_c = c\beta(\Delta\sigma/M_0)^{1/3} \tag{29}$$

where β is the shear-wave velocity near the source (assumed to be 3.75 km/s), c = 0.49 and $\Delta\sigma$ = 3 MPa.

In contrast to the smooth spectral curves in Fig. 1, real spectra calculated from noisy records of limited duration and bandwidth from earthquakes with different source-time functions and fault geometries will show fluctuating spectral amplitudes, sometime more than one corner frequency or a broad range of transition with different slopes from the displacement plateau to the final high-frequency drop-off, typically ranging between about -1 and -3 (e.g., Hartzel and Heaton, 1985; Boatwright and Choy, 1989; Polet and Kanamori, 2000; Baumbach and Bormann, 2002). Therefore, real source spectra may not be well matched by such a smooth "average" ω^{-2} source model. Nevertheless, Fig. 1 allows for the discussion of essential differences and required bandwidth ranges for reasonably reliable measurements of M_0 and E_S.

For accurate non-saturating estimates of M_0 and thus of M_w, the displacement amplitudes have to be sampled at frequencies much smaller than the corner frequency f_c, i.e., on the low-frequency asymptote plateau amplitude u_0 of the P- or S-wave source spectrum. Therefore, M_0 and M_w are not affected by the variability of the high-frequency roll-off of the spectra. Moreover, considering long and very-long periods, the calculation of M_0 is also less affected by small scale heterogeneities of the Earth structure along the travel paths and below the recording seismic stations. This allows rather precise estimates of M_w with standard deviations ≤ 0.1 m.u. (Ekström, 2007; personal communication).

In contrast, good estimates of seismic energy and thus M_e require the integration of the squared velocity amplitudes over a wide frequency range, theoretically from 0 to ∞ Hz (e.g., Haskell, 1964). However, in practice we can use only part of the spectrum, delimited by f_{min} and f_{max}. Different authors (e.g., Di Bona and Rovelli, 1988; Singh and Ordaz, 1994, Ide and Beroza, 2001) investigated the effect of the bandwidth limitations on energy estimations. Here we report the effect on M_e estimations when considering the ω^{-2} model in Fig. 1 to be roughly representative for most shallow earthquakes. In order to assess the possible influence of variations in stress drop on such estimates, the same model was applied for $\Delta\sigma$ varying in increments of one order between 0.1 and 100 MPa. The related shift of f_c for these different $\Delta\sigma$ values is shown for an earthquake with $M_w = 6.5$ in Fig. 2 and in the inset for a wider magnitude range between M_w 5.5 and 8.5.

The chosen range of variations in $\Delta\sigma$ is in agreement with the discussions in the previous sections and encompasses most of the published data (e.g., Abercrombie, 1995; Kanamori and Brodsky, 2004; Parolai et al., 2007; Venkataraman and Kanamori, 2004a). According to Fig. 2a, variations in $\Delta\sigma$ do not influence at all the displacement plateau of the source spectrum and thus estimates of M_0 as long as the basic condition of analyzing only frequencies $f << f_c$ is observed. Only if this is violated, as sometimes by established routine procedures in the case of extreme events, then also M_w may be underestimated. E.g., for the great 2004 Sumatra earthquake, values between 8.2 and 9.0 were reported by different agencies before the final value of 9.3 was established by way of special analysis (Stein and Okal, 2005; Tsai et al., 2005). In contrast, according to Eqs (18a) and (18b) and in agreement with Fig. 2b, variations in stress drop by one order are - for a given seismic moment - expected to change the released energy by one order as well and thus the estimates of M_e by almost 0.7 m.u.. Therefore, the determination of E_S and M_e requires to integrate the spectrum in a wide frequency range on both sides of the corner frequency.

When assuming that the low frequency part of the source spectrum is available, then - according to Singh and Ordaz (1994) - f_{max} should be 6 times f_c for an ω^{-2} model in order to assure that 80% of the total E_S is obtained from the integration of the source spectrum. M_e would then be underestimated only by 0.06 m.u.. This is negligible. However, the frequency range covered by f_{min} and f_{max} may cut off significant amounts of seismic enery contained both in the low- and the high-frequency part of the source spectrum, especially, if the bandwidth of integration does not cover well frequencies around f_c. In the latter case M_e may be underestimated up to a few tenths magnitude units.

Current routine procedures operate in the period ranges between 0.2-100 s (procedure according to Choy and Boatwright, 1995, applied at the US Geological Survey (USGS)) or 1-80 s (automatic near real-time procedure according to Di Giacomo et al., 2010a,b, applied by the GFZ German Research Centre for Geosciences). Table 1 summarises the magnitude-dependent underestimation of M_e, $-\Delta M_e$, based on the model used for calculating Fig. 1 but assuming variable stress drop between 0.1 and 100 MPa and integration over frequencies between 12.4 mHz and 1 Hz only. For catching nearly 100% of the energy radiated by earthquakes with magnitudes between $5.5 \leq M_w \leq 8.5$ and stress drops between $0.1 \leq \Delta\sigma \leq 100$ MPa one would need to consider frequencies between 0.001 Hz and 16 Hz. This is, however, not realistic for routine M_e estimations using teleseismic P-wave records.

Table 1. Estimates of $-\Delta M_e$, calculated for earthquakes of different moment magnitude M_w and stress drop $\Delta\sigma$ when the integration is performed only in the frequency range between 12.4 mHz and 1 Hz. For the model used see text.

$\Delta\sigma$ (MPa)	ΔM_e for $M_w = 5.5$	ΔM_e for $M_w = 6.5$	ΔM_e for $M_w = 7.5$	ΔM_e for $M_w = 8.5$
0.1	0.05	0.02	0.05	0.25
1	0.13	0.03	0.02	0.10
10	0.30	0.08	0.02	0.03
100	0.66	0.19	0.05	0.02

According to Table 1, an E_S procedure operating in the bandwidth range from 1 to 80 s may underestimate M_e up to ~0.66 m.u. for moderate ($M_w \approx 5.5$) earthquakes with very high stress drop and thus $f_c > f_{max}$. But for most earthquakes with M_w between about 6.5 and 8.5 and intermediate $\Delta\sigma$ between about 1 to 10 MPa the underestimation is expected to be < 0.1 m.u. For great earthquakes ($M_w > 8$) with $\Delta\sigma < 1$ MPa (possibly $f_c < -f_{min}$), $-\Delta M_e$ may also reach 0.2-0.3 m.u., or even more for extreme events. However, such estimates based on a simple source model, which can not account for source complexities under real conditions, must be used with caution. They can only give a rough orientation of the possible range of M_e underestimations. Underestimations for extreme events should be somewhat reduced by the more elaborate off-line USGS procedure that uses a slightly larger bandwidth and a residual integral above f_c (see Boatwright and Choy, 1986).

Besides the integration window, the calculation of E_S and M_e is mainly affected by the corrections for propagation effects and source complexities, especially at higher frequencies, which are not considered in M_w calculations. Correcting for high-frequency attenuation is one of the most challenging tasks. It requires a detailed knowledge of the velocity and attenuation structure along the propagation paths, and also especially below the seismic stations. The usually poor signal to noise ratio at frequencies higher than 1 Hz in the teleseismic range represents another big limitation, especially for moderate and small earthquakes. These combined difficulties and thus - as compared to M_0 and M_w determinations - related larger possible errors are reasons that E_S and M_e, despite their importance in assessing the damage potential of earthquakes, have rarely been used for this purpose so far.

Fig. 3a shows the station distributions for four recent earthquakes with M_w 7.6 and Fig. 3b the corresponding spectral amplitudes for four different periods between 1 and 8 s. The spectral amplitudes should show a smooth decay with distance. On average, this is reasonably well the case for all frequencies and mechanisms. This holds promise that with many good station's records available at different distances, azimuth and site conditions average estimates of E_S might be correct within a factor of about 2 to 3 (and thus M_e within about 0.2-0.3 m.u). Fig 3b reveals that, identical M_w notwithstanding, the observed spectral station amplitudes differ significantly, even when measured at nearby stations. Individual station values may scatter for the same source by a factor of 10 (Fig. 3b) due to source and propagation effects. With regard to propagation path effects, it is hoped that the rapidly increasing number of broadband stations deployed worldwide may soon allow for better accounting of the spectral amplitude attenuation along specific propagation paths and underneath individual station sites.

The influence of corrections on E_S for specific radiation patterns has been discussed by Boatwright and Choy (1986), and later by Newman and Okal (1998) and Pérez-Campos and Beroza (2001). Opinions differ especially with respect to strike-slip earthquakes, for which

E_S-M_e estimates published by the USGS tend to be systematically larger than other estimates (e.g., Di Giacomo et al., 2010a,b). Generally, corrections for source mechanism are not common for any classical magnitude such as m_B and M_S, and special investigations for short-period m_b (Schweitzer and Kværna, 1999), or E_S-M_e estimates by other authors (e.g., Newman and Okal, 1998; Di Giacomo et al., 2010a,b) yielded evidence for much smaller or negligible effects within realistically achievable data precision. In this context it is interesting to see that according to Fig. 3b source mechanism-dependent differences in the measured uncorrected spectral amplitudes between the Izmit strike-slip event and the other three thrust events appear to be significant only for the longest period here considered (8 s), but to be absent or much less for shorter periods. This may be due to the larger complexity of source radiation patterns at shorter wavelengths, which are mainly controlled by smaller scale sub-ruptures with orientations that sometimes differ significantly from that of the average overall rupture, as well as due to multi-pathing in the heterogeneous Earth's medium, which is much more pronounced for shorter wavelengths. Further, directivity may affect single station estimates of E_S by a factor 2-3 (Venkataraman and Kanamori, 2004b) or even more. For most events, such kinds of corrections on a standard routine basis are still difficult and not manageable for near real-time procedures, although they might be considered desirable for more precise research-oriented off-line data processing. In any event, more studies are required to look into the raised pros and cons of such corrections, especially how large they are, not under idealized theoretical model assumptions but rather under real complex rupture and wave propagation conditions.

Summary Discussion and Conclusions

We argue and demonstrate that the original scaling of moment magnitude M_w to seismic energy E_S via the classical Gutenberg-Richter magnitude-energy relationships is essentially arbitrary, as M_0 is only a static measure of earthquake size. Thus, M_0 carries no direct, model-independent information about the amount of seismic energy released, neither in total nor per unit of seismic moment. The ratio E_S/M_0 depends on the kinematics and dynamics of the rupture process, which are chiefly controlled by the rigidity μ of the source material, the rupture velocity V_R and the stress drop $\Delta\sigma$ in the source volume. Besides several others, these are the main parameters that govern the radiation efficiency and the frequency content of the radiated source spectrum. Therefore, the formulas for calculating M_w and M_e have been rewritten in such a way that both their relationships to classic empirical Gutenberg-Richter magnitude-energy formulas and to essential physical source parameters become more obvious at a single glance.

The mutual relationship between M_w and M_e is best expressed by the following chain of equations:

$$\boldsymbol{M_e = M_w + (\Theta + 4.7)/1.5 = M_w + [\log(E_S/M_0) + 4.7]/1.5} = M_w + [\log(\Delta\sigma/2\mu) + 4.7]/1.5 \quad (30)$$

in which 1.5 is the slope of the Gutenberg-Richter relationship between $\log E_S$ and surface-wave magnitude M_S. The left-side version of Eq. (30) reveals that $M_e = M_w$ holds only for $\Theta = \log(E_S/M_0) = \log(\Delta\sigma/2\mu) = -4.7$ and that for earthquakes according to the Kanamori condition in Eq. (5) M_e would be 0.27 m.u. larger than M_w. The versions of Eq. (30) in the middle and on the right side explain why for individual events M_e and M_w occasionally differ even more than 1 m.u. The reason is that the M_w formula has been derived by assuming $\Theta_K = \log(\Delta\sigma/2\mu) = -4.3$ = constant whereas $M_e = (\log M_0 + \Theta - 4.4)/1.5$ accepts Θ in the whole range of its variability between about $-7 < \Theta < -3$. This hints to variations in stress-drop, respectively the ratio $\Delta\sigma/2\mu$, by more than three orders of magnitude.

It is therefore that the difference between M_e and M_w be regarded as an important complementary piece of information in order to gain a more realistic and quick assessment of rupture peculiarities, and thus of the likely kind and severity of hazard associated with a given earthquake in its specific environmental context. Although a few examples have been given, many more carefully validated case studies comparing expected with really incurred effects are required before final conclusions can be drawn and recommendations be given on how to best use the difference between M_w and M_e in actual disaster management situations or long-term seismic hazard assessment schemes. In this context one should take into account that M_e tends on average to be slightly lower than M_w because Θ is in the global mean not -4.7 but more around -4.9. Therefore, larger M_e than M_w may hint already towards slightly larger than normal shaking damage potential than one would expected on the basis of M_w alone.and, if M_e-$M_w \geq 0.5$ m.u., one can for sure already expect much larger than usual devastation for the given moment magnitude, equal exposure and vulnerability conditions provided.

On the other hand, more than 0.6 m.u. smaller M_e values as compared to M_w, corresponding to $\Theta \leq -5.7$ hint to a significantly reduced relative potential for causing strong shaking damage in exposed vulnerable environs. But if such an earthquake occurs at shallow depth in a marine subduction zone and has an $M_w > 7.5$ then it is most likely a dangerous tsunami earthquake (Lomax and Michelini, 2009a). However, being aware that M_e estimates are less reliable than those of M_w and are also possibly biased up to several tenths of magnitude units for rare but with respect to size stress drop and/or rupture velocity extreme events, one should be cautious not to overrate small differences in the order of 0.2-0.3 m.u. only.

In no event should the here derived relationships between M_w and M_e be misunderstood and used for converting M_w into M_e or vice versa. It is not the average agreement between these two magnitudes but their sometimes striking difference which carries the important complementary message as highlighted with the derived formulas in this paper. Accordingly, with a view to practical applications in the context of timely warning and/or more realistic near real-time risk assessments, it is recommendable to consider only the energy-moment ratio, respectively the related M_e-M_w difference as determined with current routine procedures despite their inherent shortcomings or still disputed problems both in definition and measurement practice. Nevertheless, they permit quick rough estimates of the efficiency of an earthquake to radiate seismic wave energy. This allows, when additionally complemented by rupture duration estimates as proposed by Lomax et al. (2007), Hara (2007a, b), Bormann and Saul (2008; 2009b) or Lomax and Michelini (2009a, b), for reasonably good discrimination between earthquakes with high tsunamigenic potential and those with higher than usual potential for a given M_w to cause other types of destruction in the affected areas.

Acknowledgements
The authors acknowledge with great thanks very constructive comments and proposals made by Nicolas Deichmann, another anonymous reviewer and the journal editor on the originally submitted draft. Language-wise the revised-draft has benefited from the editing by Jeffrey de Vito. All these contributions have helped to better streamline the paper, to clarify the relationship between original assumptions made in the derivation of M_w and modern radiation efficiency considerations, and to improve the English. We are grateful also to S. Parolai for many useful discussions. Figures were drawn using the Generic Mapping Tool (GMT, Wessel and Smith, 1991) software. Domenico Di Giacomo was supported by a research grant from the European Center for Geodynamics and Seismology, Luxembourg, and was enrolled in the PhD program of the University of Potsdam, Germany, during his contribution to this study.

References

Abe, K. (1981). Magnitudes of large shallow earthquakes from 1904 to 1980, *Phys. Earth. Planet. Int.* **27**, 72-92.

Abercrombie, R. E. (1995). Earthquake source scaling relationships from -1 to 5 M_L using seismograms recorded at 22.5 km depth, *J. Geophys Res.* **100**, 24,015-24,036.

Aki, K. (1966). Generation and propagation of *G* waves from the Niigata earthquake of June 16, 1964, part 2: Estimation of earthquake moment, released energy, and stress-strain drop from the *G* wave spectrum, *Bull. Earthq. Res. Inst. Toyo Univ.* **44**, 73-88.

Aki K (1967). Scaling law of seismic spectrum, *J. Geophys. Res.* **72**, 1217-1231.

Aki K (1972). Scaling law of earthquake source time-function, *Geophys. J. R. Astr. Soc.* **31**, 3-25.

Baumbach, M., and P. Bormann (2002)..Determination of source parameters from seismic spectra, in: Bormann, P. (ed.), *IASPEI New Manual of Seismological Observatory Practice*, published by GeoForschungsZentrum Potsdam, Germany, Vol. 2, EX 3.4, 6 pp.

Beresnev, I. (2009) The reality of the scaling law of earthquake-source spectra?, *J. Seismology* **13**, 433-436, DOI 10.1007/s10950-008-9136-9.

Boatwright, J., and G. L. Choy (1986). Teleseismic estimates of the energy radiated by shallow earthquakes, *J. Geophys. Res.* **91**, 2095-2112.

Boatwright, J., and G. L. Choy (1989). Acceleration spectra for subduction zone earthquakes, *J. Geophys. Res.* **94**, B11, 15,541-15,553.

Bormann, P., and J. Saul (2008). The new IASPEI standard broadband magnitude m_B, *Seismol. Res. Lett.* **79** (5), 699-706.

Bormann, P., and J. Saul (2009a). Earthquake magnitude. In *Encyclopedia of Complexity and Systems Science*, ed. R. Meyers, *Springer*, Heidelberg-New York: vol. **3,** 2473-2496.

Bormann, P., and J. Saul (2009b). A fast, non-saturating magnitude estimator for great earthquakes, *Seism. Res. Lett.* **80**(5), 808-816; doi: 10.1785/gssrl.80.5.808.

Bormann, P., M. Baumbach, M. Bock, H. Grosser, G. L. Choy, and J. Boatwright J (2002). Seismic sources and source parameters, in: Bormann, P. (ed), IASPEI *New Manual Seismological Observatory Practice*, GeoForschungsZentrum Potsdam, Vol. 1, Chapter 3, 94 pp.

Bormann, P., R. Liu, X. Ren, R. Gutdeutsch, D. Kaiser, S. Castellaro (2007). Chinese national network magnitudes, their relation to NEIC magnitudes, and recommendations for new IASPEI magnitude standards, *Bull. Seism. Soc. Am.* **97**, 114-127.

Bormann, P., Liu R., Xu Z., Ren K., Zhang L., Wendt S. (2009). First application of the new IASPEI teleseismic magnitude standards to data of the China National Seismographic Network, *Bull. Seism. Soc. Am.* **99** (3), 1868-1891; doi: 10.1785/0120080010

Braunmiller, J., Kradolfer, U., Baer, M., and Giardini, D., 2002. Regional moment tensor determinations in the European-Mediterranian area – initial results. Tectonophysics, 356: 5-22.

Braunmiller. J., N. Deichmann, D. Giardini, S. Wiemer, and the SED Magnitude Working Group (2005). Homogeneous moment-magnitude calibration in Switzerland, *Bull. Seism. Soc. Am.* **95**,58-74.

Brune, J. N. (1970). Tectonic stress and the spectra of shear waves from earthquakes, *J. Geophys. Res.* **75**, 4997-5009.

Choy, G. L., and J. Boatwright (1995). Global patterns of radiated seismic energy and apparent stress, *J. Geophys. Res.* **100**, 18,205-18,228.

Choy, G. L., and S. Kirby (2004). Apparent stress, fault maturity and seismic hazard for normal-fault earthquakes at subduction zones, *Geophys. J. Int.* **159**, 991-1012.

Choy, G. L., A. McGarr, S. H. Kirby, and J. Boatwirght (2006). An overview of the global variability in radiated energy and apparent stress, in: Abercrombie R. , A. McGarr, H.

Kanamori (eds): Radiated energy and the physics of earthquake faulting, *AGU Geophys. Monogr. Ser.* **170**, 43-57.

Di Bona, M., and A. Rovelli (1988). Effects of bandwidth limitation on stress drop estimated from integrals of the ground motion, *Bull. Seism. Soc. Am.* **78**, 1818-1825.

Di Giacomo, D., S. Parolai, P. Bormann, H. Grosser, J. Saul, R. Wang, and J. Zschau (2010a). Suitability of rapid energy magnitude estimations for emergency response purposes, *Geophys. J. Int.*, **180**, 361-374, doi: 10.1111/j.1365-246X.2009.04416.x.

Di Giacomo, D., S. Parolai, P. Bormann, H. Grosser, J. Saul, R. Wang, and J. Zschau (2010b). Erratum to "Suitability of rapid energy magnitude estimations for emergency response purposes", *Geophys. J. Int.*, 181, 1725-1726, doi: 10.1111/j.1365-246X.2010.04610.x.

Duda, S., and D. Kaiser (1989). Spectral magnitudes, magnitude spectra and earthquake quantification; the stability issue of the corner period and of the maximum magnitude for a given earthquake, *Tectonophysics* **166**, 205-219.

Dziewonski, A. M., T. A. Chou, and J. H. Woodhouse (1981). Determination of earthquake source parameters from waveform data for studies of global and regional seismicity. *J. Geophys. Res.* **86**, 2:2825-2852

Eshelby, J. D. (1969). The elastic field of a crack extending non-uniformly under general anti-plane loading, *J. Mech. Phys. Solids* **8**, 100-104.

Grünthal, G., and R. Wahlström (2003). An M_w based earthquake catalogue for central, northern and northwestern Europe using a hierarchy of magnitude conversions, *J. Seismol.* **7**, 507-531.

Grünthal, G., R. Wahlström, and D. Stromeyer (2009). The unified catalogue of earthquakes in central, northern, and northwestern Europe (CENEC) – updated and expanded to the last millennium, *J. Seismol.* **13**, 517-541; doi: 10.1007/s10950-008-9144-9.

Gutenberg, B. (1945a). Amplitude of surface waves and magnitude of shallow earthquakes, Bull. Seism. Soc. Am. **35**, 3-12.

Gutenberg ,B. (1945b). Amplitudes of P, PP, and S and magnitude of shallow earthquakes, Bull. Seism. Soc. Am. **35**, 57-69.

Gutenberg, B. (1945c). Magnitude determination of deep-focus earthquakes, *Bull. Seism. Soc. Am***.** **35**, 117-130.

Gutenberg, B., and C. F. Richter (1956a). Magnitude and energy of earthquakes, *Annali di Geofisica* **9**, 1-15.

Gutenberg, B., and C. F. Richter (1956b). The energy of earthquakes, *Q. J. Geol. Soc. London* **17**, 1-14.

Hanks, C., and H. Kanamori (1979). A moment magnitude scale, *J Geophys Res* **84**, 2348-2350.

Hara, T. (2007a). Measurement of the duration of high-frequency energy radiation and its application to determination of the magnitudes of large shallow earthquakes, *Earth Planets Space* **59**, 227-231.

Hara, T. (2007b). Magnitude determination using duration of high frequency radiation and displacement amplitude: application to tsunami earthquakes, *Earth. Planet Space* **59**, 561-565.

Hartzel, S. H., and T. Heaton (1985). Teleseismic time functions for large, shallow subduction zone earthquakes, *Bull. Seism. Soc. Am.* **75**(4), 965-1004.

Haskell, N. A. (1964). Total energy and energy spectral density of elastic wave radiation from propagating faults, *Bull. Seism. Soc. Am.* **54**(6), 1811-1841.

Houston, H. (1999). Slow ruptures, roaring tsunamis, *Nature* **400**, 409-410

Houston H., and H. Kanamori (1986) Source spectra of great earthquakes: teleseismic constraints on rupture process and strong motion. *Bull. Seism. Soc. Am.* **76**, 19-42

Husseini, M. I. (1977). Energy balance for formation along a fault, *Geophys. J. Roy. Astron. Soc.* **49**, 699-714.

IASPEI (2005) Summary of Magnitude Working Group recommendations on standard procedures for determining earthquake magnitudes from digital data. http://www.iaspei.org/commissions/CSOI.html

Ide, S., and G. C Beroza (2001),. Does apparent stress vary with earthquake size? *Geophys. Res. Lett.* ***28***(17), 3349-3352.

Kanamori, H. (1972) Mechanism of tsunami earthquakes. Phys Planet Earth Inter 6: 346-359

Kanamori, H (1977) The energy release in great earthquakes J Geophys Res 82:2981-2987.

Kanamori, H. (1978). Quantification of earthquakes, *Nature* **271**(2), 411-414.

Kanamori, H. (1983). Magnitude scale and quantification of earthquakes, *Tectonophysics* **93**, 185-199.

Kanamori, H. (2006). The radiated energy of the 2004 Sumatra-Andaman earthquake, in: Abercrombie R, McGarr A, Kanamori H (eds): Radiated energy and the physics of earthquake faulting, *AGU Geophys Monogr Ser* **170**, 59-68.

Kanamori, H., and D. L. Anderson (1975). Theoretical basis of some empirical relations in seismology, *Bull. Seism Soc. Am.* **65**(5),1073-1095

Kanamori, H., and M. Kikuchi (1993). The 1992 Nicaragua earthquake: a slow tsunami earthquake associated with subducted sediments, *Nature* **361**, 714-716.

Kanamori, H., and E. E. Brodsky (2004). The physics of earthquakes, *Rep Prog Phys* **67**, 1429-1496; doi: 10.1088/0034-4885/67/8/R03.

Kanamori, H., and L. Rivera (2004). Static and dynamic scaling relations for earthquakes and their implications for rupture speed and stress drop, *Bull. Seism. Soc. Am.* **94**(1), 314-319.

Kikuchi, M., and H. Kanamori (1994). The mechanism of the deep Bolivia earthquake of June 9, 1994, *Geophys. Res. Lett.* **21**(22), 2341-2344.

Knopoff, L. (1958). Energy release in earthquakes, *Geophys. J.* **1,** 44-52.

Kostrov, B. V. (1966). Unsteady propagation of longitudinal shear cracks, *J. Appl. Math. Mech.* (Engl. transl.)**30,** 1241-1248. .

Kostrov, B. V. (1974). Seismic moment and energy of earthquakes, and seismic flow of rock, *Izv. Acad. Sci. USSR, Phys. Solid Earth* (English Transl) **1**, 23-40.

Krüger, F., and M. Ohrnberger (2005). Tracking the rupture of the M_w = 9.3 Sumatra earthquake over 1,150 km at teleseismic distances, *Nature* **435**, 937-939, doi: 10.1038/nature03696.

Kwiatek, G., K. Plenkers, M. Nakatani, Y. Yabe, G. Dresen, and JAGUAR-Group (2010). Frequency-magnitude characteristics down to magnitude -4.4 for induced seismicity recorded at Mponeng Gold Mine, South Africa, *Bull. Seism. Soc. Am.***100**(3), 11.65-1173; doi: 10.1785/0120090277.

Lomax, A. , and A. Michelini (2009a). M_{wpd}: A duration-amplitude procedure for rapid determination of earthquake magnitude and tsunamigenic potential from *P* waveforms, *Geophys. J. Int.* **176**, 200-214 ; doi: 10.1111/j.1365-246X.2008.03974.x .

Lomax, A., and A. Michelini (2009b). Tsunami early warning using earthquake rupture duration, *Geophys. Res. Lett.* **36,** L09306, doi:10000.1029/2009GL037223.

Lomax, A., A. Michelini, and A. Piatanesi (2007). An energy-duration procedure for rapid and accurate determination of earthquake magnitude and tsunamigenic potential, *Geophys. J. Int.* **170**, 1195-1209; DOI: 10.1111/j.1365-246X.2007.03469.x.

Newman, A. V., and E. A. Okal (1998). Teleseismic estimates of radiated seismic energy: The E/M_0 discriminant for tsunami earthquakes, *J. Geophys. Res.*, **103**, 26,885-26,897.

Okal, E. A., and J. Talandier (1989). M_m: A variable period mantle magnitude, *J. Geophys. Res.* **94**, 4169-4193.

Orowan, E. (1960). Mechanisms of seimic faulting in rock deformation: a symposium, *Geol. Soc. Am. Mem.* **79**, 323-345.

Papazachos, B. C., A. A. Kiratzi, and B. G. Karacostas (1997). Towards a homogeneous moment-magnitude determination for earthquakes in Greece and the surrounding area, *Bull. Seism. Soc. Am.* **87**, 474-483.

Parolai, S., D. Bindi, E. Durukal, H. Grosser, C. Milkereit (2007). Source parameter and seismic moment-magnitude scaling for northwestern Turkey, *Bull. Seim. Soc. Am.* **97**(2), 655-660.

Péres-Campos, X., and G. C. Beroza (2001). An apparent mechanism dependence of radiated seismic energy, *J. Geophys. Res.* **106** (B6), 11,127-11,136.

Polet, J., and H. Kanamori (2000). Shallow subduction zone earthquakes and their tsunamigenic potential, *Geophys. J. Int.* **142**, 684-702.

Polet, J., and H. K. Thio (2003). The 1994 Java tsunami earthquake and its “normal” aftershocks, *Geophys. Res. Lett.* **30**(9), 1474, doi:10.1029/2002GL016806.

Polet, J., and Kanamori (2009). Tsunami earthquakes. In Ecyclopedia of Complexity and Systems Science, vol. 10, ed. R. Meyers, 9,577-9,592.

Richter, C. (1935). An instrumental earthquake magnitude scale, *Bull. Seism. Soc. Am*. **25**, 1-32

Richter, C. (1958). Elementary seismology. *W.H. Freeman Comapany*, San Francisco and London, 768 pp.

Ristau, J., G. C. Rogers, and J. F. Cassidy (2005) Moment magnitude-local magnitude calibration for earthquakes in Western Canada, Bull. Seism. Soc. Am. **95**, 1994-2000.

Savage, J. C., and M. D. Wood (1971). The relation between apparent stress and stress drop, *Bull. Seism. Soc. Am.* **61**, 1381-1388.

Schweitzer, J., and T. Kværna (1999). Influence of source radiation patterns on globally observed short-period magnitude estimates (mb), *Bull. Seism. Soc. Am.* **89**(2), 342-347.

Scordilis, E. M. (2006). Empirical global relations converting M_S and m_b to moment magnitude, *J. Seismol.* **10**, 225-236.

Singh, S. K., and M. Ordaz (1994). Seismic energy release in Mexican subductiion zone earthquakes, *Bull. Seism. Soc. Am.* **84**(5), 1533-1550.

Stein, S., and E. A. Okal (2005). Speed and size of the Sumatra earthquake, *Nature* **434**, 581-582; doi: 10.1038/434581a.

Stromeyer, D., G. Grünthal, and R. Wahlstrom (2004). Chi-square regression for seismic strength parameter relations, and their uncertainties, with applications to an *M*w based earthquake catalogue for central, northern and northwestern Europe, *J. Seismol.* **8**(1), 143–153.

Tsai, V. C., M. Nettles, G. Ekström, and A. Dziewonski (2005). Multiple CMT source analysis of the 2004 Sumatra earthquake, *Geophysical Research Letters* **32**; L17304, doi: 10.1029/2005GL023813.

Vassiliou, M. S., and H. Kanamori (1982). The energy release in earthquakes, *Bull. Seism. Soc. Am.* **72**, 371-387.

Venkataraman, A, and H. Kanamori (2004a). Observational constraints on the fracture energy of subduction zone earthquakes, *J. Geophys. Res.* **109**, B04301, doi: 0431.01029JB002549.

Venkataraman, A., and H. Kanamori (2004b), Effect of directivity on estimates of radiated seismic energy, *J. Geophys. Res. 109*, B04301, doi:10.1029/2003JB002548.

Weinstein, S. A., and E A Okal (2005). The mantle wave magnitude M_{m} and the slowness parameter Θ: Five years of real-time use in the context of tsunami warning, *Bull. Seism. Soc. Am.* **95**, 779-799; doi: 10.1785/0120040112

Wessel, P., and W. H. F. Smith (1991). Free software helps map and display data, *Eos Trans. AGU* **72**(41*)*, 441, 445-446.

Wyss, M., and J. N. Brune (1968). Seismic moment, stress, and source dimensions for earthquakes in the California-Nevada region, *J. Geophys. Res.* **73**, 4681-4694.

Yadav, R. B. S., P. Bormann, B. K. Rastogi, and M. C Chopra (2009). A homogeneous and complete earthquake catalog for northeast India and the adjoining region, *Seism. Res. Lett.* **80** (4), 598-616.

GFZ German Research Center for Geosciences
Division 2: Physics of the Earth
Telegrafenberg
D-14473 Potsdam, Germany
(P.B., D. D.G.)

FIGURE CAPTIONS

Fig. 1. a) Far-field "source spectra" of ground displacement amplitudes *A* for a seismic shear source model (see text) as a function of frequency *f*, scaled to seismic moment M_0 and the equivalent moment magnitude M_w and **b)** the same for ground motion velocity amplitudes *V*, scaled to seismic moment rate and M_w. Note that the maximum seismic energy $E_S \sim V^2$ is radiated around f_c. The arrows point to the frequencies at which the classical narrow-band magnitudes m_b and $M_S(20)$ are measured. The horizontal bars cover the period range for measuring the IASPEI (2005) recommended broadband magnitude m_B for body-waves and M_S(BB) for Rayleigh surface waves. Copy of Fig. 1 in Bormann et al. (2009, p. 1870), with © granted by the Seismological Society of America.

Fig. 2. a) Far-field displacement and **b)** velocity source spectra scaled to seismic moment and moment rate, respectively, for model earthquake with $M_w = 6.5$ but different stress-drop $\Delta\sigma$ in units of MPa. The inset in Fig. 2b shows the variation of f_c, obtained according to Eq. (29), in a wider range of M_w for $\Delta\sigma$ varying in increments of one order between 0.1 and 100 MPa.

Fig. 3. a) Global distributions of seismic stations which recorded four $M_w = 7.6$ earthquakes (plotted with their GCMT fault plane solutions); b) Spectral amplitudes measured at periods of 1, 2, 4 and 8 s, at stations between 20° and 98° epicentral distance. The color of the "beach-balls" corresponds with the color of the station symbols and measured spectral amplitudes; blue inverted triangles: 1999-07-17 Izmit strike-slip earthquake; red triangles: 2001-01-26 India earthquake; black circles: 2002-09-08 Papua New Guinea earthquake; magenta diamonds: 2005-10-08 Pakistan earthquake. The latter three earthquakes are thrust events. There is no obvious mechanism-dependent level-trend in the spectral amplitudes.

Click here to download high resolution image

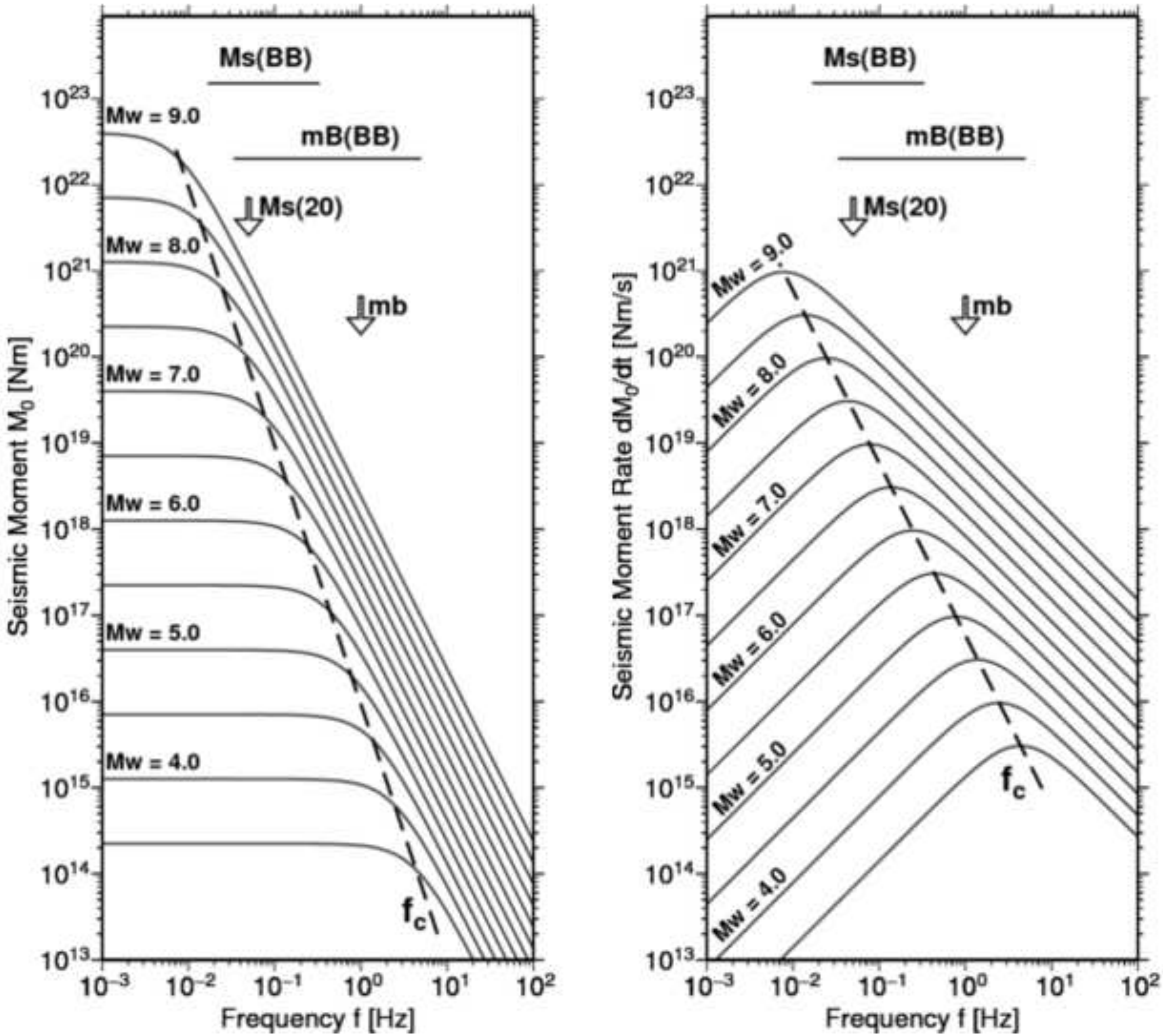

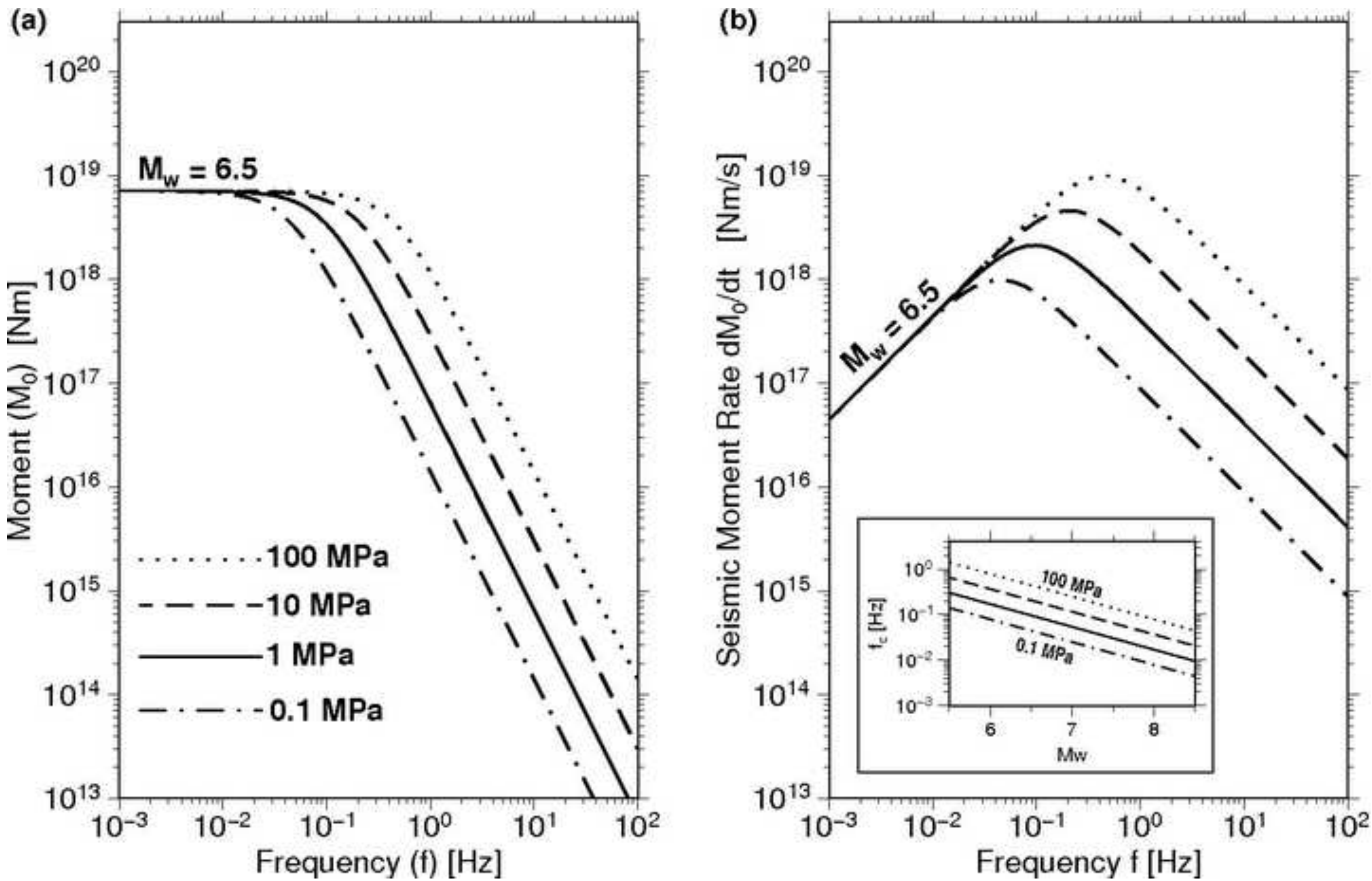
(a)
(b)
$M_w = 6.5$
Moment (M_0) [Nm]
Frequency (f) [Hz]
100 MPa
10 MPa
1 MPa
0.1 MPa
Seismic Moment Rate dM_0/dt [Nm/s]
Frequency f [Hz]
f_c [Hz]
Mw
100 MPa
0.1 MPa

Click here to download high resolution image